Published in final edited form as:
Cell Host Microbe. 2014 December 10; 16(6): 748–758. doi:10.1016/j.chom.2014.10.018.

Modulation of RNA polymerase II phosphorylation downstream of pathogen perception orchestrates plant immunity

Fangjun Li[1,2,11], **Cheng Cheng**[3,11], **Fuhao Cui**[1,2,11], **Marcos V. V. de Oliveira**[2,3,4,11], **Xiao Yu**[2], **Xiangzong Meng**[3], **Aline C. Intorne**[2,4], **Kevin Babilonia**[3,5], **Maoying Li**[1,3], **Bo Li**[2], **Sixue Chen**[6], **Xiaofeng Ma**[7], **Shunyuan Xiao**[7], **Yi Zeng**[8], **Zhangjun Fei**[8], **Richard Metz**[9], **Charles D. Johnson**[9], **Hisashi Koiwa**[10], **Wenxian Sun**[1], **Zhaohu Li**[1], **Gonçalo A. de Souza Filho**[4], **Libo Shan**[2,*], and **Ping He**[3,*]

[1]College of Agronomy and Biotechnology, China Agricultural University, Beijing 100193, China

[2]Department of Plant Pathology & Microbiology, and Institute for Plant Genomics & Biotechnology, Texas A&M University, College Station, TX 77843, USA

[3]Department of Biochemistry & Biophysics, and Institute for Plant Genomics & Biotechnology, Texas A&M University, College Station, TX 77843, USA

[4]Center of Biosciences & Biotechnology, Darcy Ribeiro State University of Northern of Rio de Janeiro, 28013-602, Brazil

[5]Department of Biology, University of Puerto Rico, Mayagüez Campus, Mayagüez, PR 00680, USA

[6]Department of Biology, University of Florida, Gainesville, Florida 32610, USA

[7]Institute for Bioscience & Biotechnology Research, University of Maryland, Rockville, MD 20850, and Department of Plant Science & Landscape Architecture, University of Maryland, College Park, MD 20742, USA

[8]Boyce Thompson Institute, Cornell University, Ithaca, NY 14853, USA

[*]Correspondence: lshan@tamu.edu (L.S.), pinghe@tamu.edu (P.H.).
[11]Co-first author

The authors have declared no conflict of interests.

Supplemental Information: Supplemental Information includes seven figures, seven tables and Supplemental Experimental Procedures.

Author contributions: F.L. performed biochemical assays of CPL3, CTD, CDKC and MAPK activities, and analyzed CDKC plants; C.C performed phenotypic analysis and cloning of *aggie1*, RNA-seq analysis, and VIGS assays; F.C. performed screen, phenotypic analysis, cloning and NGS of *aggie3*; M.O. sequenced candidate genes of *Aggie1*, and performed RNA-seq analysis and CDKC plants; X.Y. generated *mpk6RNAi* plants and performed CDKC and CTD phosphorylation in these plants; X. Meng performed MAPK phosphorylation on CDKCs; A.I. sequenced candidate genes of *Aggie1*; K.B. screened *aggie1*; M.L. performed Y2H assay; B.L. generated *mpk6RNAi* plants and validated MAPK inhibitor and MKP; S.C. performed MS assay; X. Ma and S.X. performed powdery mildew assay; Y.Z. and Z.F. analyzed RNA-seq data; R.M. and C.J. performed NGS; H.K. provided reagents; W.S., Z.L., and G.S.F. analyzed data; L.S and P.H. generated mutant population, designed experiments, analyzed data, and wrote the paper with inputs from other authors.

[9]Genomics and Bioinformatics Services, Texas A&M AgriLife Research, College Station, TX 77843, USA

[10]Department of Horticultural Sciences, Texas A&M University, College Station, TX 77843, USA

Summary

Perception of microbe-associated molecular patterns (MAMPs) elicits host transcriptional reprogramming as part of the immune response. Although pathogen perception is well studied, the signaling networks orchestrating immune gene expression remain less clear. In a genetic screen for components involved in the early immune gene transcription reprogramming, we identified *Arabidopsis* RNA polymerase II C-terminal domain (CTD) phosphatase-like 3 (CPL3) as a negative regulator of immune gene expression. MAMP perception induced rapid and transient cyclin-dependent kinase (CDKC)-mediated phosphorylation of *Arabidopsis* CTD. The CDKCs, which are in-turn phosphorylated and activated by a canonical MAP kinase (MAPK) cascade, represent a point of signaling convergence downstream of multiple immune receptors. CPL3 directly dephosphorylated CTD to counteract MAPK-mediated CDKC regulation. Thus, modulation of the phosphorylation dynamics of eukaryotic RNA polymerase II transcription machinery by MAPKs, CTD kinases and phosphatases constitutes an essential mechanism for rapid orchestration of host immune gene expression and defense upon pathogen attacks.

Introduction

Plants and animals possess pattern recognition receptors (PRRs) to detect the presence of microbes by recognizing microbe-associated molecular patterns (MAMPs) (Boller and Felix, 2009). In plants, MAMPs are usually perceived by cell surface-resident PRRs and elicit pattern-triggered immunity (PTI). *Arabidopsis* FLS2, a leucine-rich repeat receptor-like kinase (LRR-RLK), recognizes a conserved 22-amino acid peptide (flg22) from bacterial flagellin (Boller and Felix, 2009). Upon flagellin perception, FLS2 rapidly associates with another LRR-RLK BAK1, thereby initiating downstream signaling (Chinchilla et al., 2007; Heese et al., 2007; Sun et al., 2013). BAK1 also heteromerizes with several PRRs, including EFR (receptor for bacterial elongation factor EF-Tu) (Roux et al., 2011) and AtPEPR1 (receptor for endogenous danger signal PEP1) (Postel et al., 2010). BIK1, a plasma membrane-resident receptor-like cytoplasmic kinase in the FLS2/BAK1 complex, is rapidly phosphorylated upon flg22 perception to transduce intracellular signaling (Lin et al., 2014; Lu et al., 2010; Zhang et al., 2010). BIK1 is able to phosphorylate NADPH oxidase family member RBOHD (respiratory burst oxidase homolog D), thereby contributing to the production of reactive oxygen species (ROS) (Kadota et al., 2014; Li et al., 2014). Rapid activation of convergent MAP kinases (MAPKs) and calcium-dependent protein kinases downstream of multiple PRRs is followed with the expression of MAMP responsive genes (Tena et al., 2011). It appears that distinct MAMPs elicit massive overlapping transcriptional reprogramming (Zipfel et al., 2006). Several transcription factors, especially members of WRKY and ERF families, could be directly phosphorylated by MAPKs and are potentially involved in defense gene regulation (Meng and Zhang, 2013). Yet, the molecular signaling networks leading to the rapid reprogramming of immune genes have remained elusive.

Transcription of protein-coding genes in eukaryotes is intricately orchestrated by RNA polymerase II (RNAPII), general transcription factors, mediators and gene-specific transcription factors. The multi-subunit RNAPII is evolutionarily conserved from yeast to human. Its largest subunit Rpb1 contains a carboxyl-terminal domain (CTD) consisting of conserved heptapeptide repeats with the consensus sequence $Y_1S_2P_3T_4S_5P_6S_7$ (Buratowski, 2009). The number of repeats varies from 26 in yeast, 34 in *Arabidopsis*, to 52 in mammals (Hajheidari et al., 2013). The combinatorial complexity of CTD posttranslational modifications constitutes a "CTD code" that is "read" by CTD binding proteins to regulate the transcription cycle, modify chromatin structure, and modulate RNA capping, splicing, and polyadenylation. In particular, the CTD undergoes waves of serine phosphorylation and dephosphorylation events regulated by various CTD kinases, often members of cyclin-dependent kinases (CDKs), and phosphatases during transcription initiation, elongation and termination. The interplay between different CTD kinases and phosphatases provides a means for coupling and coordinating specific stages of transcription by recruiting other factors required for proper gene expression (Buratowski, 2009).

Although both immune signaling mechanisms and CTD phosphorylation cycles in regulating gene transcription have been studied separately, whether and how they are connected remains enigmatic. Here, we demonstrate that CTD phosphorylation dynamics plays a key role in regulating host immunity. *Arabidopsis* RNAPII CTD exhibits rapid and transient phosphorylation dynamics upon perception of different MAMPs. Moreover, biochemical and genetic analyses uncovered an immune gene regulation circuit in *Arabidopsis* by MAPK-mediated phosphorylation of CTD kinases CDKCs upon flagellin perception. A genetic screen for components involved in the early immune gene transcription reprogramming identified *Arabidopsis CPL3* (CTD phosphatase-like 3) as a negative regulator of immune gene expression and immunity to pathogen infections. *Arabidopsis* CPL3 is a homolog of yeast Fcp1 (TFIIF-associating CTD phosphatase) (Koiwa et al., 2002). The *Arabidopsis* genome encodes 4 CPLs, and CPL1 and CPL3 were uncovered from a genetic screen for hyper-induction of plant abiotic stress response gene *RD29A* promoter (Koiwa et al., 2002). Our biochemical analyses indicate that CPL3 interacts with and preferentially dephosphorylates Ser2 of RNAPII CTD to counter-regulate MAPK/CDKC-mediated CTD phosphorylation. Thus, our study suggests that modulation of general transcription machinery phosphorylation is a key feature of host immune response.

Results

Enhanced immune gene activation and disease resistance in *aggie1* and *aggie3* mutants

To elucidate the signaling networks regulating immune gene activation, we developed a genetic screen with an ethyl methanesulfonate (EMS)-mutagenized population of *Arabidopsis* transgenic plants expressing a luciferase reporter gene under the control of the *FRK1* promoter (*pFRK1::LUC*). *FRK1* (flg22-induced receptor-like kinase 1) is a specific and early marker gene activated by multiple MAMPs, likely downstream of MAPKs (Asai et al., 2002; He et al., 2006). A series of mutants with altered *pFRK1::LUC* activity upon flg22 treatment were identified and named as *Arabidopsis* genes governing immune gene expression (*aggie*). Two *aggie* mutants, *aggie1* and *aggie3* (*aggie3* was found to be allelic

with *aggie1* after map-based cloning), exhibited enhanced *FRK1* promoter activity compared to wild-type (WT) *pFRK1:∷LUC* transgenic plants at various time points after flg22 treatment (Fig. 1A & 1B). Notably, the *aggie1* and *aggie3* mutants did not significantly activate the *FRK1* promoter (0.8∼2 fold) in the absence of flg22, suggesting specific regulation of *FRK1* expression by *Aggie* in immune signaling. The *aggie1* mutants also potentiated *pFRK1:∷LUC* activity in response to elf18, an 18-amino acid peptide of bacterial EF-Tu, and fungal chitin (Fig. 1C & S1A), suggesting that the mutation in *aggie1* likely occurs in a convergent component downstream of multiple MAMP receptors. In addition, the *pFRK1:∷LUC* activation by a nonpathogenic bacterium *Pseudomonas syringae* pv. *tomato* DC3000 (*Pst*) *hrcC*, which is deficient in delivery of type III effectors, and by a non-adaptive bacterium *P. syringae* pv. *phaseolicola* NPS3121 was also enhanced in *aggie1* and *aggie3* mutants (Fig. 1D). The *aggie1* and *aggie3* mutants were more resistant to virulent *Pst* and *P. syringae* pv. *maculicola* ES4326 (*Psm*) infections (Fig. 1E, S1B & S1C). The bacterial population in *aggie1* and *aggie3* mutants was about five to ten-fold less than that in WT plants 4 days post inoculation (dpi) with *Psm* (Fig. 1E). A ten-fold reduction in bacterial growth was also observed in *aggie1* mutant when *Pst* was inoculated upon dipping inoculation (Fig. S1B). The disease symptom development was less pronounced in *aggie1* mutant than WT plants (Fig. S1C). However, the flg22-induced MAPK activation detected by an α-pERK antibody was not affected in *aggie1* mutant compared to WT plants (Fig. 1F). Similarly, the *aggie1* mutant exhibited normal oxidative burst and BIK1 phosphorylation in response to flg22 treatment (Fig. 1G & S1D). These results suggest that Aggie1 functions either downstream or independently of MAPK activation and ROS production in FLS2 signaling.

Aggie1 and *Aggie3* encode a plant CTD phosphatase-like protein

Genetic analysis of F1 plants from a backcross *of aggie1* to *pFRK1:∷LUC* plants indicated that *aggie1* is a recessive mutation (Fig. 2A). We crossed the *aggie1* mutant (in the Col-0 background) with the *Ler* accession and mapped *aggie1* to Chromosome 2 between markers F4P9-3 and T1B8-2 that are 110 kb apart (Fig. S2A). Sequencing the individual genes within this region identified a G to A mutation located 1294 bp downstream of the predicted start codon of *At2g33540*. The mutation occurred at the 3′ splice site of the 4th intron, resulting in a potential alternative 3′ acceptor site located 43 bp downstream (Fig. 2B & S2B). The mutation in *aggie3* was identified by map-based cloning coupled with next generation sequencing. The *aggie3* carries a G to A mutation at position 962 bp of *At2g33540*, located at the 3′ splice site of the 2nd intron, which results in one base pair shift of the 3′ acceptor site. The predicted transcripts of *aggie1* and *aggie3* were confirmed by Sanger sequencing of cDNA products (Fig. S2B). *At2g33540* encodes CPL3 with an N-terminal domain of unknown function, an FCPH (Fcp homology) domain and a BRCT (breast cancer 1 C terminus) domain (Bang et al., 2006; Koiwa et al., 2002). The *aggie1* and *aggie3* mutants were also named as *cpl3-5* and *cpl3-6*, respectively. The mutations in *aggie1/cpl3-5* and *aggie3/cpl3-6* resulted in truncated proteins lacking both FCPH and BRCT domains (Fig. 2B). To confirm that the *aggie1* phenotypes were caused by mutation in *CPL3*, we introduced *CPL3* under the control of its native promoter into *aggie1*. The *FRK1* promoter activity in response to flg22 treatment was restored to the WT level in three independent complementation lines (Fig. 2C). In addition, similar to *aggie1* mutants, two

CPL3 T-DNA insertion lines *cpl3-3* and *cpl3-4*, but not *cpl2-2* (Ueda et al., 2008), were more resistant to *Psm* infection than WT plants (Fig. 2D). Interestingly, *aggie1/cpl3-5* and *cpl3-4* plants also showed enhanced resistance to an obligate biotrophic fungal pathogen, *Golovinomyces cichoracearum* UCSC1, with 5-7 fold reduction in mildew spores on the inoculated leaf surface compared to WT plants (Fig. 2E). Quantitative reverse transcription-polymerase chain reaction (qRT-PCR) analysis indicated that endogenous *FRK1* expression was elevated in *cpl3-4* and *aggie1/cpl3-5* mutants (Fig. 2F). The expression of another MAMP marker gene *WRKY30* was also enhanced in *cpl3-4* and *aggie1/cpl3-5* mutants (Fig. 2F). Taken together, the results indicate that CPL3 plays a negative role in immune gene regulation and plant immunity.

Global regulation of immune gene expression by CPL3

To determine transcriptome dynamics regulated by CPL3 during elicitation of immune responses, we performed RNA sequencing (RNA-seq) analysis of Col-0 WT and *cpl3-3* mutant treated without or with flg22 for 30 min. The correlation coefficient (r) for the expression profile of each detectable transcript in WT and *cpl3-3* seedlings without flg22 treatment is close to linear (0.98) (Fig. 3A). Among 24074 detectable transcripts, 93 showed reduced and 227 showed enhanced expression [fold change ≥ 2 and false discovery rate (FDR) < 0.05] in *cpl3-3* mutant compared to that in WT plants without treatment (Table S1), suggesting that CPL3 does not appear to control general gene transcription. Using a cut-off of fold change ≥ 2 and FDR < 0.05, we identified 964 flg22-induced genes in WT and 1128 in *cpl3-3* with 918 genes induced in both WT and *cpl3-3*, 46 induced only in WT and 210 induced only in *cpl3-3* (Fig. 3B & Table S2). Hierarchical clustering analysis of differential flg22-induced genes in WT and *cpl3-3*, which were defined as CPL3-dependent flg22-induced genes, classified them into four groups, Group I: CPL3-required flg22-induced genes (genes induced in WT, but not in *cpl3-3*, 46 genes); Group II: CPL3-potentiated flg22-induced genes (genes induced in both WT and *cpl3-3* with at least 1.5 fold higher induction in WT than *cpl3-3*, 32 out of 918 genes); Group III: CPL3-attenuted flg22-induced genes (genes induced in both WT and *cpl3-3* with at least 1.5 fold higher induction in *cpl3-3* than WT, 180 out of 918 genes); Group IV: CPL3-suppressed flg22-induced genes (genes induced in *cpl3-3*, but not in WT, 210 genes) (Fig. 3C & Table S3). Thus, among 468 CPL3-dependent flg22-induced genes, 390 (83%) showed increased flg22-induction (Group III & IV) whereas 78 (17%) exhibited reduced flg22-induction (Group I & II) in *cpl3-3* compared to WT. Notably, a large portion of CPL3-dependent flg22-induced genes are classified to be associated with defense responses (Table S3 & S4). Enrichment analysis of Gene Ontology (GO) indicates that among 180 CPL3-attenuted flg22-induced genes (Group III), the frequency of genes associated with biotic stress, innate immune response, response to bacterium and fungus, and salicylic acid (SA)-mediated signaling pathway was significantly enriched compared to the predicated frequency in the genome (Fig. 3D & Table S4). Many defense-related transcription factors, such as WRKYs and ERFs, and RLKs were also overrepresented in Group III genes (Table S3). The genes encoding flg22-activated MKK4 and MPK11 were highly induced in *cpl3-3* compared to WT. Interestingly, *cpl3-3* also displayed the increased expression of genes encoding PROPEP1 and PROPEP3, the precursors of elicitor peptide PEPs, which function as endogenous damage-associated molecular pattern to amplify danger signals during pathogen infection (Liu et al., 2013). The

elevated expression of several flg22-induced genes, including *At1g07160*, *At1g51920*, *At1g59860*, and *At2g17740* in *cpl3-3* and *aggie1/cpl3-5* mutants was confirmed with qRT-PCR analysis (Fig. 3E). Collectively, the data suggest that CPL3 plays a negative role in regulating a large subset of flg22-induced genes. Apparently, CPL3-regulated genes did not show significant correlation with SA, ethylene, methyl jasmonate (MeJA) and ABA-responsive genes (Fig. S3). Among 101 flg22 down-regulated genes in WT and *cpl3-3* (fold change ≥ 2 and FDR < 0.05), only 2 genes showed > 2-fold difference between WT and *cpl3-3*, suggesting that CPL3 does not appear to significantly control flg22-reduced genes (Table S5).

CTD phosphorylation dynamics in PTI signaling

With the FCPH domain, CPLs are hypothesized to regulate gene transcription via modulating the phosphorylation status of RNAPII CTD in the nucleus. When expressed in *Arabidopsis* protoplasts, CPL3-GFP was observed in the nucleus, which is likely mediated by a nuclear localization signal (NLS) at its N terminus (Fig. S4A). To reveal the potential involvement of CTD phosphorylation in plant immunity, we cloned CTD of *Arabidopsis* RNAPII and expressed it in protoplasts. Significantly, flg22 treatment induced a rapid mobility shift of CTD as early as 2 min post-treatment (Fig. 4A). The flg22-induced mobility shift could be removed by calf alkaline intestinal phosphatase (CIP) treatment (Fig. 4B), suggesting the involvement of phosphorylation in flg22-induced CTD modification. The elf18 and chitin treatments also induced CTD mobility shift (Fig. 4C). The flg22 treatment also induced the mobility shift of CTD fused with NLS (NLS-CTD) (Fig. S4B).

Interestingly, flg22 treatment was able to induce CTD phosphorylation at Ser sites as detected by specific antibodies recognizing pSer2, pSer5 or pSer7 (Fig. 4A). In addition, flg22 treatment induced Ser2, Ser5 and Ser7 phosphorylation of endogenous CTD of RNAPII in *Arabidopsis* seedlings treated with flg22 for different lengths of time (Fig. 4D). The phosphorylation intensity peaked between 10 and 30 min and gradually declined 60 min after treatment. The phosphorylation modification was confirmed by CIP treatment which diminished the signal detected with α-pSer2 antibody (Fig. S4C). Together, these data indicate that the rapid and transient phosphorylation of CTD upon flg22 perception may constitute an important step in plant immune signaling.

MAPKs phosphorylate CDKCs in flg22 signaling

CPL3 is predicted to be a CTD Ser2 phosphatase since its yeast homolog Fcp1 preferentially dephosphorylates Ser2 (Koiwa et al., 2002). CTD Ser2 is phosphorylated by cyclin-dependent kinases CDK9 and CDK12 in mammals (Bartkowiak et al., 2010). We examined the potential involvement of *Arabidopsis* orthologs CDKC;1 and CDKC;2 in CTD phosphorylation (Cui et al., 2007). The flg22 treatment induced a mobility shift of CDKC;1 (Fig. 5A), which could be removed by phosphatase CIP treatment (Fig. 5B), suggesting that CDKC;1 was phosphorylated upon flg22 treatment. CDKC;2 exhibited multiple bands in the absence of flg22 treatment (Fig. 5A). Consistent with the activation of CDKs by cyclins, co-expression of CYCT1;3, the partner of CDKCs (Cui et al., 2007), also resulted in two bands of CDKC;1, similar to that after flg22 treatment (Fig. S5A). The data suggest that *Arabidopsis* CDKCs are activated upon flg22 perception.

MAPK cascades act as a convergent point mediating multiple MAMP-triggered signaling. The flg22-induced mobility shift of CDKC;1 was blocked by a MAPK inhibitor PD184161 (Fig. 5C & S5B) and by co-expression of MAPK-specific phosphatase MKP (Fig. 5D & S5B), suggesting that activation of MAPKs by flg22 leads to CDKC phosphorylation. MPK3, MPK4, MPK6 and MPK11 have been shown to be activated by flg22 treatment (Meng and Zhang, 2013). We tested whether these MAPKs could directly phosphorylate CDKCs. The FLAG epitope-tagged MAPK was expressed in protoplasts (Fig. S5C), activated by flg22 treatment, and then immunoprecipitated with α-FLAG antibody for an *in vitro* kinase assay with GST-CDKC as a substrate. The flg22-activated MPK3 complex strongly phosphorylated both GST-CDKC; 1 and GST-CDKC;2 (Fig. 5E). Consistently, the *in vitro* kinase assay with purified MPK proteins also indicated that activated MPK3 directly phosphorylated GST-CDKC; 1 and GST-CDKC;2 (Fig. 5F & S5D). Activated MPK6 also phosphorylated GST-CDKC; 1 and GST-CDKC;2 *in vitro* (Fig. 5F), suggesting potential redundancy of MPK3 and MPK6 in controlling CDKC activity. Notably, MPK3 and MPK6 interacted with CDKC;1 and CDKC;2, but not CYCT1;3, in protoplast co-immunoprecipitation (Co-IP) assays (Fig. 5G, S5E & S5F). Sequence analysis of CDKCs identified two potential MAPK phosphorylation sites (Ser/Thr followed by Pro) S94 and S259 (Sorensson et al., 2012). Exchange of S94, but not S259, to Ala, blocked flg22-induced CDKC;1 mobility shift and suppressed CDKC;2 mobility shift (Fig. S5G). Importantly, the CDKC;1^{S94A} and CDKC;2^{S94A} mutants were no longer phosphorylated by activated MPK3 and MPK6 *in vitro* (Fig. 5F). Furthermore, mass spectrometry (MS) analyses identified the phosphorylation of S94 in both CDKC;1 and CDKC;2 phosphorylated by MPK3 or MPK6 (Fig. 5H, S5H, S5I & S5J). The data support that MPK3 and MPK6 phosphorylate CDKCs at S94.

CDKCs are MAPK-activated CTD kinases

To test whether the flg22-induced MAPK cascade could activate CDKC kinase activity towards CTD, we first activated MBP-CDKCs with MPK3 immunoprecipitated from flg22-treated protoplasts. The activated MBP-CDKC proteins were used for a kinase assay with GST-CTD as a substrate. The phosphorylation of CTD was detected by α-pSer2, α-pSer5 and α-pSer7 antibodies. MPK3-activated CDKC;1 or CDKC;2 phosphorylated CTD at three Ser residues (Fig. 6A & S6A). Both CDKC;1^{S94A} and CDKC;2^{S94A}, which were no longer able to be phosphorylated by MAPKs, were compromised in their ability to phosphorylate CTD (Fig. 6B). Similar with the activation of CDKs by cyclins, immunoprecipitated CDKCs with CYCT1;3 could also phosphorylate CTD at Ser2, Ser5 and Ser7 residues (Fig. 6C & 6D). These data indicate that CDKCs are authentic CTD kinases and their activity is regulated by an flg22-induced MAPK cascade.

CPL3 dephosphorylates CDKC-mediated CTD phosphorylation

We next examined whether CPL3 possesses CTD phosphatase activity. We purified MBP fusion proteins of full-length CPL3, N-terminal CPL3 (CPL3N) and C-terminal CPL3 (CPL3C) and performed *in vitro* phosphatase assays with GST-CTD that was phosphorylated by CDKC;1/CYCT1;3 (Fig. 6C) or CDKC;2/CYCT1;3 (Fig. 6D & S6B). CPL3 was able to dephosphorylate pSer2, pSer5 and pSer7 *in vitro* with a preference for pSer2 (Fig. 6C, 6D & S6B). CPL3C with both the FCPH and BRCT domains, but not FCPH

alone nor CPL3N, carries the phosphatase activity that completely dephosphorylated CTD pSer2 and partially dephosphorylated pSer5 and pSer7 (Fig. 6C & 6D). Our results suggested that both FCPH and BRCT domains are required for CPL3 phosphatase activity. We further tested the potential interaction between CPL3 and CTD. An *in vitro* pull-down assay indicated that GST-CTD could pull down CPL3. The interaction between CPL3 and CTD was markedly enhanced when CTD was phosphorylated (Fig. 6E). Further analyses with different domains of CPL3 indicated that both FCPH and BRCT domains were required for the interaction (Fig. S6C & S6D). The interaction between CPL3C and CTD was confirmed with yeast two-hybrid assay (Fig. 6F). These results are consistent with the finding that yeast Fcp1 predominantly dephosphorylates pSer2 and requires both FCPH and BRCT domains for its catalytic activity (Ghosh et al., 2008).

Structural and mutational analyses of yeast Fcp1 defined essential conserved residues within the FCPH domain (Ghosh et al., 2008). We mutated some of these conserved residues in CPL3, including D933 (corresponding to Fcp1D258), K1046 (Fcp1K280) and D1064D1065 (Fcp1D297D298) to Ala, and tested their phosphatase activity. All these mutants were still able to interact with CTD in an *in vitro* pull-down assay (Fig. S6E). D933A and D1064AD1065A (DD1064AA) rendered a complete loss of CPL3 catalytic activity (Fig. 6G). Similarly, expression of WT CPL3C, but not D933A mutant, reduced flg22-induced *pFRK1-LUC* induction in *cpl3-4* mutant protoplasts, suggesting the functional importance of D933 (Fig. S6F). Surprisingly, the K1046A mutation did not affect CPL3 activity (Fig. 6G). Given that the corresponding residue K280 in Fcp1 was suggested to participate in transition-state stabilization by binding to acylphosphate intermediate during CTD dephosphorylation (Ghosh et al., 2008), our data suggest that K1046 in CPL3 might not be essential for stabilizing the transition state, and that CPL3 has a similar but distinct requirement for catalytic activity compared to Fcp1.

We further compared Ser2, Ser5 and Ser7 phosphorylation level of endogenous CTD in WT and *cpl3-4* seedlings. The overall Ser2 phosphorylation level was enhanced in the *cpl3-4* mutant compared to WT plants with and without flg22 treatment (Fig. 6H). In contrast, the level of Ser5 and Ser7 phosphorylation appears to be similar in WT and *cpl3-4* seedlings (Fig. 6H). This is consistent with *in vitro* analysis that CPL3 preferentially dephosphorylates Ser2 of CTD.

CDKCs positively regulate plant innate immunity

We tested the potential involvement of CDKCs in CTD phosphorylation and plant immunity. The *cdkc;2-1* (SALK_149280) mutant has undetectable full-length transcripts (Fig. S7A & S7B), whereas the available T-DNA insertion lines of *cdkc;1* (SALK_148550 & SALK_091405) remained similar transcript levels as WT plants. We generated *CDKC;1* RNA interference (RNAi) plants with reduced expression of *CDKC;1* transcripts (Fig. S7C). Consistent with CDKCs being CTD kinases, the flg22-induced phosphorylation of Ser2, Ser5 or Ser7 of CTD was reduced in *cdkc;1RNAi* and *cdkc;2* mutant plants (Fig. 7A & S7D). Similarly, the *cdkc;1RNAi* and *cdkc;2* plants showed reduced induction of MAMP marker genes, including *FRK1*, *WRKY30*, *PP2C* (*At1g07160*) and *At1g51920* upon flg22 treatment compared to WT plants (Fig. 7B). In addition, the *cdkc;1RNAi* and *cdkc;2* mutant

plants were more susceptible to virulent *Pst* infection than WT plants as indicated by 5-8 fold increase of bacterial growth in the mutants (Fig. 7C). The bacterial growth of type III deficient *Pst hrcC* was also increased in the *cdkc;1RNAi* or *cdkc;2* mutants (Fig. 7C). The increased growth of *Psm* was also observed in *cdkc;2* mutant (Fig. S7E). CDKC;1 and CDKC;2 play redundant roles in plant growth and development, and resistance to virus infections (Cui et al., 2007). Therefore, we generated double mutants by silencing *CDKC;1* in the *cdkc;2* mutant using virus-induced gene silencing (VIGS). The *cdkc;2/cdkc;1VIGS* plants displayed wrinkled leaves 3 weeks after VIGS and exhibited retarded growth 4 weeks after VIGS (Fig. S7F). We performed the pathogen infection assays before the growth defects clearly appeared. Similar with RNAi plants, the *cdkc;1VIGS* plants showed reduced induction of *FRK1* and *WRKY30* upon flg22 treatment, and the reduction seemed to be further exacerbated in *cdkc;2/cdkc;1VIGS* plants compared to plants silenced with a vector control (Fig. S7G). Consistently, the *cdkc;1VIGS* mutant plants were more susceptible to *Pst* infection with about 5-10 fold increase of bacterial growth than control plants (Fig. 7D). Notably, bacterial population in the *cdkc;2/cdkc;1VIGS* plants was about 100-fold higher than that in control plants (Fig. 7D). Together, these data indicate that CDKC;1 and CDKC;2 are positive regulators in plant immunity to bacterial infections.

To further investigate the involvement of MPK3 and MPK6 in flg22-induced CTD and CDKC phosphorylation, we generated estradiol inducible *MPK6* RNAi transgenic plants in *mpk3* mutant. The protein level of MPK6 was markedly reduced in *mpk3/MPK6RNAi* plants after estradiol treatment (Fig. S7H). Importantly, the flg22-induced CTD Ser2, Ser5 and Ser7 phosphorylation was diminished in the *mpk3/MPK6RNAi* plants compared to WT plants (Fig. 7E). Furthermore, the flg22-induced CDKC;1 mobility shift was blocked in the *mpk3/MPK6RNAi* plants (Fig. 7F), providing genetic evidence of MPK3 and MPK6 in flg22-induced CDKC;1 and CTD phosphorylation.

Discussion

We have demonstrated that the phosphorylation dynamics of the RNAPII core transcription machinery is regulated by the evolutionarily conserved kinases and phosphatases in response to pathogen attacks. Specifically, we revealed a MAMP-induced phosphorylation relay emanating from a MAPK cascade downstream of multiple PRRs to CDKCs and RNAPII CTD that activates the transcription machinery for immune gene expression. We also elucidated dephosphorylation of RNAPII CTD by CPL3 phosphatase as a counter-regulatory mechanism to fine tune transcriptional reprogramming for appropriate immune responses. Thus, both CDKCs and CPL3 target RNAPII CTD and oppositely regulate plant immune gene expression and disease resistance to bacterial and fungal pathogens (Fig. 7G). Considering the conservation of MAPKs and CTD kinases and phosphatases among eukaryotes, the immune signaling circuits identified in this study may represent an evolutionarily convergent regulatory mechanism that eukaryotic cells use to promptly respond to extracellular stimuli.

As an element of the core transcription machinery, RNAPII is subject to complex regulation that ensures proper processing of nascent mRNAs. The phosphorylation dynamics of RNAPII CTD has been extensively studied, in particular in yeast, and many CTD binding

proteins and transcription events are associated with specific CTD phosphorylation patterns (Buratowski, 2009). A universal CTD cycle has been proposed to orchestrate the transcription of virtually all genes through complex interplay between different kinases, phosphatases and other modifying enzymes (Bataille et al., 2012). However, the manner in which specific cellular responses regulate CTD phosphorylation dynamics, which in turn controls gene expression, has been a mystery. We show here that MAMP perception markedly induces rapid and transient CTD phosphorylation on various Ser residues in its heptad repeats. This phosphorylation is achieved by a direct phosphorylation relay from a MAPK cascade to CDKCs and counter-regulated by the CPL3 phosphatase. The data suggest an important role of MAPK-mediated RNAPII CTD phosphorylation in transcriptional regulation of plant immune genes.

CPL3 belongs to a member of multigene family in *Arabidopsis* (Koiwa et al., 2002; Koiwa et al., 2006). Only CPL3 and CPL4 contain both FCPH and BRCT domains, whereas CPL1 and CPL2 contain FCPH and double-stranded RNA-binding domains. The *cpl1* mutants display altered expression of cold-, salt-, ABA-, and osmotic stress-inducible genes, and *cpl3* mutants show specific alternation to ABA responses (Jiang et al., 2013; Koiwa et al., 2002). Despite lacking the BRCT domain, CPL1 could specifically dephosphorylate Ser5 of *Arabidopsis* CTD (Koiwa et al., 2004). In addition, CPL1 dephosphorylates RNA binding protein HYPONASTIC LEAVES 1 (HYL1) to regulate processing and strand selection during plant miRNA biogenesis (Manavella et al., 2012). CPL3 is a prototype Fcp1 phosphatase containing both FCPH phosphatase catalytic domain and BRCT domain. Our results support that CPL3 is a genuine CTD Ser2 phosphatase and requires both FCPH and BRCT domains for its activity, which is similar to yeast Fcp1. However, distinct from *Fcp1*, *CPL3* is not an essential gene. *CPL4*, the closest homolog of *CPL3*, is likely an essential gene involved in plant vegetative growth and development (Bang et al., 2006). Therefore, it appears that CPL4 is involved in the regulation of RNAPII activity for general transcription, whereas CPL3 specifically regulates RNAPII activity during plant stress responses. It remains unknown how CPL3 activity is regulated upon MAMP treatment. It is possible that CPL3 could be activated by upstream kinases or other regulators in MAMP signaling. Additionally, CPL3 may interact with specific transcription factors to regulate immune gene expression.

CDKs are often activated by phosphorylation of conserved Thr residues within the T-loops by CDK-activating kinases (CAKs). A plant specific CDK, CDKF;1 phosphorylates the T-loops of CDKDs and activates their kinase activity towards CTD (Hajheidari et al., 2012). Here, we identified the activation of CDKCs by flg22-induced MAPK cascade. *In vivo* and *in vitro* data provide evidence that MPK3 directly phosphorylates CDKC;1 and CDKC;2, and activates CDKC kinase activity towards CTD. In fission yeast, CTD Ser2 phosphorylation is elevated under nitrogen starvation condition, which depends on a stress-responsive MAPK pathway (Sukegawa et al., 2011). In human T-cell receptor and phorbal ester signaling, MAPKs are involved in phosphorylation of CDK9 to enhance HIV transcription (Mbonye et al., 2013). Apparently, activation of CDKs by MAPK cascades might be a conserved mechanism for the regulation of RNAPII CTD phosphorylation.

Experimental Procedures

Plant growth, generation of *pFRK1::LUC* transgenic plants and mutant screens

Arabidopsis accession Col-0, *Ler*, *pFRK1::LUC* wild-type (WT) and mutant (*aggie*) transgenic plants, *cpl2-2* (SALK_059753), *cpl3-3* (SALK_094720C), *cpl3-4* (SALK_051322C), *cdkc;2-1* (SALK_149280C) and *fls2* were grown in pots containing soil (Metro Mix 360) in a growth room at 23°C, 60% relative humidity and 75μE $m^{-2}s^{-1}$ light with a 12-hr photoperiod. To detect CTD phosphorylation and gene induction, one-week-old or 12-day-old seedlings grown on ½ MS medium were transferred to water for overnight and then treated with 100 nM flg22 for indicated time points.

The *pFRK1::LUC* construct in protoplast transient expression vector (He et al., 2006) was sub-cloned into a binary vector *pCB302* and introduced into *Arabidopsis* Col-0 plants. The transgenic plants were selected with Basta resistance and analyzed with flg22-induced *pFRK1::LUC* expression. The seeds of homozygous *pFRK1::LUC* transgenic plants were mutagenized by 0.4% EMS. Approximately 6,000 M2 seedlings were grown on liquid ½ MS medium for 14 days, transferred to water for overnight and then treated with 10 nM flg22. The individual seedlings were transferred to each well of 96-well plate 12 hr after flg22 treatment and sprayed with 0.2 mM luciferin. The plate was put in the dark for 20 min, and the bioluminescence signal was read by a luminometer (Perkin Elmer). The putative mutants were transferred to solid ½ MS medium for additional 10 days and then transferred to soil to set seeds.

Plasmid construction

The *CTD*, *CDKC;1*, *CDKC;2*, *CYCT1;3*, *CPL3*, *CPL3N*, *CPL3*C and *CPL3FCPH* genes were amplified from Col-0 cDNA library with primers containing BamHI or NcoI at N terminus and StuI at C terminus, and introduced into a plant expression vector *pHBT* with an HA or FLAG epitope-tag at C terminus. The point mutations of $CDKC;1^{S94A}$, $CDKC;1^{S259A}$, $CDKC;2^{S94A}$, $CDKC;2^{S259A}$ and different *CPL3C* mutants were generated by site-directed mutagenesis. A 400-bp fragment of *CDKC;1* was amplified from Col-0 cDNA with primers containing EcoRI at N terminus and KpnI at C terminus,, and inserted into VIGS *pYL156* (*pTRV-RNA2*) vector by EcoRI and KpnI digestion. The *CDKC;1* RNAi construct was obtained from Dr. Z. Chen (Cui et al., 2007). The primers for cloning and point mutations were listed in the Supplemental Experimental Procedures. The *CDKC;1* and *CDKC;2* were sub-cloned into a modified GST fusion protein expression vector pGEX4T-1 (Pharmacia) or a modified pMAL-c2 vector (New England BioLabs) with BamHI and StuI digestion and different *CPL3* constructs were sub-cloned into a modified pMAL-c2 vector with SpeI or BamHI and StuI digestion. The recombinant CDKC and CPL3 fusion protein expression vectors were introduced into *E. coli* strain BL21 (DE3). Expression of fusion proteins and affinity purification were performed with standard protocol. The *CPL3N*, *CPL3*C and *FCPH* genes were sub-cloned into a modified *pGBKT7* vector (Clontech) with SpeI or BamHI and StuI digestion, and the *CTD* gene was sub-cloned into a modified *pGADT7* vector (Clontech) with BamHI and StuI digestion for yeast two-hybrid assay. The constructs of *GST-CTD*, *pCPL3::CPL3*, MAPK fusion protein and protoplast expression

vectors were reported previously (He et al., 2006; Koiwa et al., 2002; Koiwa et al., 2004). The MAPK-specific phosphatase (MKP) was cloned from mouse (Kovtun et al., 1998).

Pathogen infections, NGS, RNA-seq, kinase assay, CTD phosphorylation and dephosphorylation, VIGS, Co-IP and MS assays are listed in Supplemental Experimental Procedures.

Supplementary Material

Refer to Web version on PubMed Central for supplementary material.

Acknowledgments

We thank Salk Institute and ABRC for the *Arabidopsis* T-DNA insertion lines, Dr. Zhixiang Chen for CDKC and CYCT fusion protein and RNAi constructs, Dr. Shuqun Zhang for MPK fusion protein constructs, Dr. Keiko Torii for *pTK103* vector, Dr. Ning Zhu for technical assistance of MS analysis, Drs. Greg Martin and Paul de Figueiredo for critical reading of the manuscript. The work was supported by NIH (R01GM092893) and NSF (IOS-1252539) to P.H and NIH (R01GM097247) and the Robert A. Welch foundation (A-1795) to L.S. The NGS was supported by Texas AgriLife Genomics Seed Grant. F. L. and F. C. were partially supported by China Scholarship Council. M.V.V.O and A.C.I. were partially supported by Rio de Janeiro State Research Foundation (FAPERJ), Brazil. K.B. was supported by NSF REU program.

References

Asai T, Tena G, Plotnikova J, Willmann MR, Chiu WL, Gomez-Gomez L, Boller T, Ausubel FM, Sheen J. MAP kinase signalling cascade in Arabidopsis innate immunity. Nature. 2002; 415:977–983. [PubMed: 11875555]

Bang W, Kim S, Ueda A, Vikram M, Yun D, Bressan RA, Hasegawa PM, Bahk J, Koiwa H. Arabidopsis carboxyl-terminal domain phosphatase-like isoforms share common catalytic and interaction domains but have distinct in planta functions. Plant Physiol. 2006; 142:586–594. [PubMed: 16905668]

Bartkowiak B, Liu P, Phatnani HP, Fuda NJ, Cooper JJ, Price DH, Adelman K, Lis JT, Greenleaf AL. CDK12 is a transcription elongation-associated CTD kinase, the metazoan ortholog of yeast Ctk1. Genes Dev. 2010; 24:2303–2316. [PubMed: 20952539]

Bataille AR, Jeronimo C, Jacques PE, Laramee L, Fortin ME, Forest A, Bergeron M, Hanes SD, Robert F. A universal RNA polymerase II CTD cycle is orchestrated by complex interplays between kinase, phosphatase, and isomerase enzymes along genes. Mol Cell. 2012; 45:158–170. [PubMed: 22284676]

Boller T, Felix G. A renaissance of elicitors: perception of microbe-associated molecular patterns and danger signals by pattern-recognition receptors. Annu Rev Plant Biol. 2009; 60:379–406. [PubMed: 19400727]

Buratowski S. Progression through the RNA polymerase II CTD cycle. Mol Cell. 2009; 36:541–546. [PubMed: 19941815]

Chinchilla D, Zipfel C, Robatzek S, Kemmerling B, Nurnberger T, Jones JD, Felix G, Boller T. A flagellin-induced complex of the receptor FLS2 and BAK1 initiates plant defence. Nature. 2007; 448:497–500. [PubMed: 17625569]

Cui X, Fan B, Scholz J, Chen Z. Roles of Arabidopsis cyclin-dependent kinase C complexes in cauliflower mosaic virus infection, plant growth, and development. Plant Cell. 2007; 19:1388–1402. [PubMed: 17468259]

Ghosh A, Shuman S, Lima CD. The structure of Fcp1, an essential RNA polymerase II CTD phosphatase. Mol Cell. 2008; 32:478–490. [PubMed: 19026779]

Hajheidari M, Farrona S, Huettel B, Koncz Z, Koncz C. CDKF;1 and CDKD Protein Kinases Regulate Phosphorylation of Serine Residues in the C-Terminal Domain of Arabidopsis RNA Polymerase II. Plant Cell. 2012; 24:1626–1642. [PubMed: 22547781]

Hajheidari M, Koncz C, Eick D. Emerging roles for RNA polymerase II CTD in Arabidopsis. Trends Plant Sci. 2013; 18:633–643. [PubMed: 23910452]

He P, Shan L, Lin NC, Martin GB, Kemmerling B, Nurnberger T, Sheen J. Specific bacterial suppressors of MAMP signaling upstream of MAPKKK in Arabidopsis innate immunity. Cell. 2006; 125:563–575. [PubMed: 16678099]

Heese A, Hann DR, Gimenez-Ibanez S, Jones AM, He K, Li J, Schroeder JI, Peck SC, Rathjen JP. The receptor-like kinase SERK3/BAK1 is a central regulator of innate immunity in plants. Proc Natl Acad Sci U S A. 2007; 104:12217–12222. [PubMed: 17626179]

Jiang J, Wang B, Shen Y, Wang H, Feng Q, Shi H. The Arabidopsis RNA Binding Protein with K Homology Motifs, SHINY1, Interacts with the C-terminal Domain Phosphatase-like 1 (CPL1) to Repress Stress-Inducible Gene Expression. PLoS Genet. 2013; 9:e1003625. [PubMed: 23874224]

Kadota Y, Sklenar J, Derbyshire P, Stransfeld L, Asai S, Ntoukakis V, Jones JD, Shirasu K, Menke F, Jones A, et al. Direct Regulation of the NADPH Oxidase RBOHD by the PRR-Associated Kinase BIK1 during Plant Immunity. Mol Cell. 2014

Koiwa H, Barb AW, Xiong L, Li F, McCully MG, Lee BH, Sokolchik I, Zhu J, Gong Z, Reddy M, et al. C-terminal domain phosphatase-like family members (AtCPLs) differentially regulate Arabidopsis thaliana abiotic stress signaling, growth, and development. Proc Natl Acad Sci U S A. 2002; 99:10893–10898. [PubMed: 12149434]

Koiwa H, Bressan RA, Hasegawa PM. Identification of plant stress-responsive determinants in Arabidopsis by large-scale forward genetic screens. J Exp Bot. 2006; 57:1119–1128. [PubMed: 16513815]

Koiwa H, Hausmann S, Bang WY, Ueda A, Kondo N, Hiraguri A, Fukuhara T, Bahk JD, Yun DJ, Bressan RA, et al. Arabidopsis C-terminal domain phosphatase-like 1 and 2 are essential Ser-5-specific C-terminal domain phosphatases. Proc Natl Acad Sci U S A. 2004; 101:14539–14544. [PubMed: 15388846]

Kovtun Y, Chiu WL, Zeng W, Sheen J. Suppression of auxin signal transduction by a MAPK cascade in higher plants. Nature. 1998; 395:716–720. [PubMed: 9790195]

Li L, Li M, Yu L, Zhou Z, Liang X, Liu Z, Cai G, Gao L, Zhang X, Wang Y, et al. The FLS2-Associated Kinase BIK1 Directly Phosphorylates the NADPH Oxidase RbohD to Control Plant Immunity. Cell Host Microbe. 2014; 15:329–338. [PubMed: 24629339]

Lin W, Li B, Lu D, Chen S, Zhu N, He P, Shan L. Tyrosine phosphorylation of protein kinase complex BAK1/BIK1 mediates Arabidopsis innate immunity. Proc Natl Acad Sci U S A. 2014; 111:3632–3637. [PubMed: 24532660]

Liu Z, Wu Y, Yang F, Zhang Y, Chen S, Xie Q, Tian X, Zhou JM. BIK1 interacts with PEPRs to mediate ethylene-induced immunity. Proc Natl Acad Sci U S A. 2013; 110:6205–6210. [PubMed: 23431184]

Lu D, Wu S, Gao X, Zhang Y, Shan L, He P. A receptor-like cytoplasmic kinase, BIK1, associates with a flagellin receptor complex to initiate plant innate immunity. Proc Natl Acad Sci U S A. 2010; 107:496–501. [PubMed: 20018686]

Manavella PA, Hagmann J, Ott F, Laubinger S, Franz M, Macek B, Weigel D. Fast-forward genetics identifies plant CPL phosphatases as regulators of miRNA processing factor HYL1. Cell. 2012; 151:859–870. [PubMed: 23141542]

Mbonye UR, Gokulrangan G, Datt M, Dobrowolski C, Cooper M, Chance MR, Karn J. Phosphorylation of CDK9 at Ser175 enhances HIV transcription and is a marker of activated P-TEFb in CD4(+) T lymphocytes. PLoS Pathog. 2013; 9:e1003338. [PubMed: 23658523]

Meng X, Zhang S. MAPK cascades in plant disease resistance signaling. Annu Rev Phytopathol. 2013; 51:245–266. [PubMed: 23663002]

Postel S, Kufner I, Beuter C, Mazzotta S, Schwedt A, Borlotti A, Halter T, Kemmerling B, Nurnberger T. The multifunctional leucine-rich repeat receptor kinase BAK1 is implicated in Arabidopsis development and immunity. Eur J Cell Biol. 2010; 89:169–174. [PubMed: 20018402]

Roux M, Schwessinger B, Albrecht C, Chinchilla D, Jones A, Holton N, Malinovsky FG, Tor M, de Vries S, Zipfel C. The Arabidopsis leucine-rich repeat receptor-like kinases BAK1/SERK3 and BKK1/SERK4 are required for innate immunity to hemibiotrophic and biotrophic pathogens. Plant Cell. 2011; 23:2440–2455. [PubMed: 21693696]

Sorensson C, Lenman M, Veide-Vilg J, Schopper S, Ljungdahl T, Grotli M, Tamas MJ, Peck SC, Andreasson E. Determination of primary sequence specificity of Arabidopsis MAPKs MPK3 and MPK6 leads to identification of new substrates. Biochem J. 2012; 446:271–278. [PubMed: 22631074]

Sukegawa Y, Yamashita A, Yamamoto M. The fission yeast stress-responsive MAPK pathway promotes meiosis via the phosphorylation of Pol II CTD in response to environmental and feedback cues. PLoS Genet. 2011; 7:e1002387. [PubMed: 22144909]

Sun Y, Li L, Macho AP, Han Z, Hu Z, Zipfel C, Zhou JM, Chai J. Structural basis for flg22-induced activation of the Arabidopsis FLS2-BAK1 immune complex. Science. 2013; 342:624–628. [PubMed: 24114786]

Tena G, Boudsocq M, Sheen J. Protein kinase signaling networks in plant innate immunity. Curr Opin Plant Biol. 2011; 14:519–529. [PubMed: 21704551]

Ueda A, Li P, Feng Y, Vikram M, Kim S, Kang CH, Kang JS, Bahk JD, Lee SY, Fukuhara T, et al. The Arabidopsis thaliana carboxyl-terminal domain phosphatase-like 2 regulates plant growth, stress and auxin responses. Plant Mol Biol. 2008; 67:683–697. [PubMed: 18506580]

Zhang J, Li W, Xiang T, Liu Z, Laluk K, Ding X, Zou Y, Gao M, Zhang X, Chen S, et al. Receptor-like cytoplasmic kinases integrate signaling from multiple plant immune receptors and are targeted by a Pseudomonas syringae effector. Cell Host Microbe. 2010; 7:290–301. [PubMed: 20413097]

Zipfel C, Kunze G, Chinchilla D, Caniard A, Jones JD, Boller T, Felix G. Perception of the bacterial PAMP EF-Tu by the receptor EFR restricts Agrobacterium-mediated transformation. Cell. 2006; 125:749–760. [PubMed: 16713565]

Highlights

- RNA polymerase II CTD phosphatase (CPL3) mutants show enhanced immune gene activation
- MAMPs induce cyclin-dependent kinases CDKCs and RNA pol II CTD phosphorylation
- Direct CDKC phosphorylation by MAP kinase (MAPK) activates immune gene expression
- CPL3 counteracts MAPK-CDKC regulation via RNA pol II CTD dephosphorylation

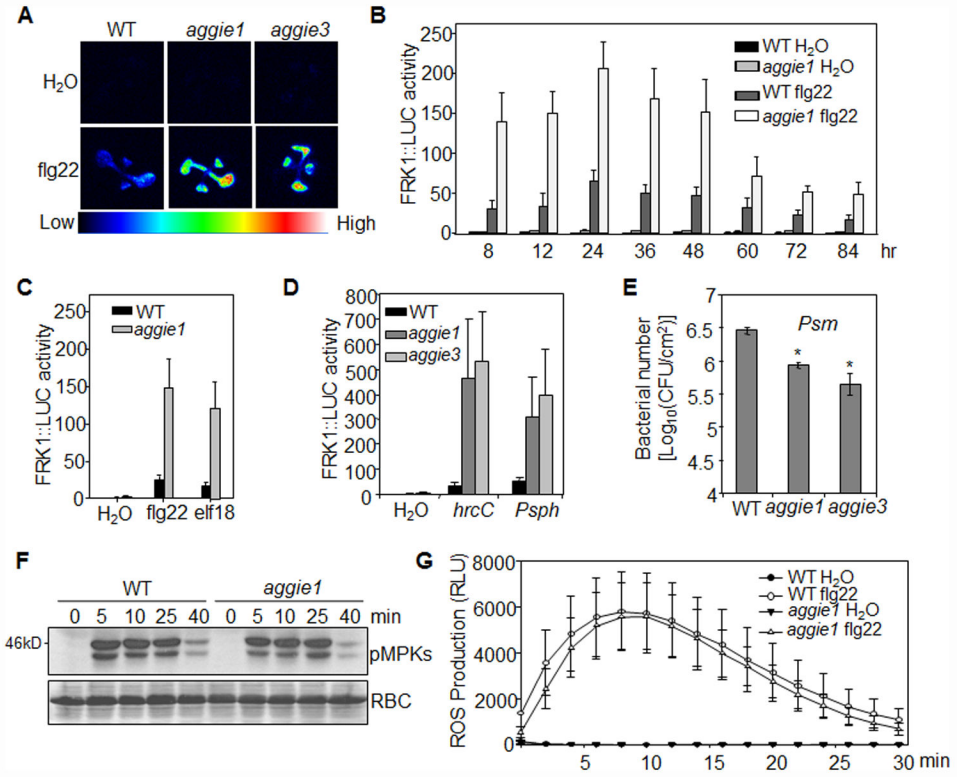

Figure 1. Elevated *pFRK1::LUC* expression and disease resistance in *aggie1* and *aggie3* mutants

(A) Luciferase activity in 10-day-old *pFRK1::LUC* (WT), *aggie1 and aggie3* seedlings. Seedlings were treated with or without 10 nM flg22 for 12 hr and photographed with an EMCCD camera. **(B)** Time-course of *pFRK1::LUC* activity. The seedlings were treated with 100 nM flg22 over 84 hr. The data are shown as means ± se from at least 6 seedlings for each time point. **(C)** The *pFRK1::LUC* activity triggered by different MAMPs. Ten-day-old seedlings were treated with 100 nM flg22 or elf18 for 15 hr. **(D)** The *pFRK1::LUC* activity triggered by different bacteria. Four-week-old plants were hand-inoculated with *hrcC* or *Psph* at OD_{600} = 0.5. The data are shown as means ± se from at least 8 leaves for each treatment 15 hpi. **(E)** Elevated disease resistance to *Psm* infection in *aggie* mutants. Four-week-old plants were hand-inoculated with *Psm* at $OD_{600}=5 \times 10^{-4}$. The data are shown as means ± se with Student's *t*-test. * indicates $p<0.05$ compared to WT. **(F)** flg22-induced MAPK activation. Twelve-day-old seedlings were treated with 100 nM flg22 for different time points. MAPK activation was analyzed with an α-pERK antibody (top panel), and protein loading was shown by Coomassie brilliant blue (CBB) (bottom panel) staining for RuBisCO (RBC). **(G)** flg22-trigered ROS burst. Leaf discs were treated with H_2O or 100 nM flg22 over 30 min. The data are shown as means ± se from 40 leaf discs.

The above experiments were repeated 4 times with similar results (see also Figure S1).

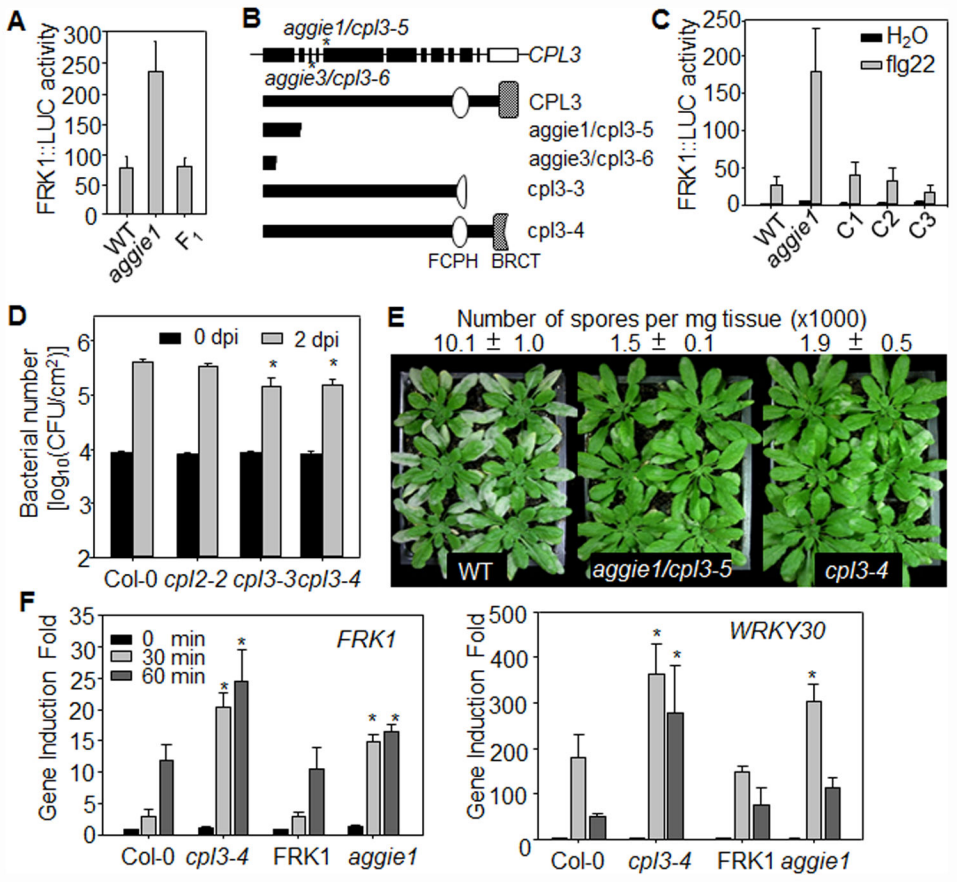

Figure 2. *Aggie1* and *Aggie3* encode CPL3, a regulator of plant immunity

(A) *aggie1* is a recessive mutation. Ten-day-old F1 seedlings derived from a cross between *aggie1* and WT *pFRK1:LUC* were treated with 100 nM flg22 for 12 hr. The data are shown as means ± se from at least 5 seedlings. **(B)** The scheme of the *CPL3* genomic DNA and deduced protein domains. The top panel is a schematic illustration of the *CPL3* genomic DNA with exons (solid box), intron (lines) and 3′ untranslated region (open box). The stars indicate the mutations in *aggie1/cpl3-5* and *aggie3/cpl3-6.* The other panels illustrate the protein domain structures of CPL3 and four truncated mutants. **(C)** Complementation analysis. C1, C2 and C3 are three independent transgenic lines of *aggie1* complemented with *pCPL3:CPL3.* Ten-day-old seedlings were treated with 100 nM flg22 for 12 hr. The data are shown as means ± se from at least 10 seedlings. **(D)** The *cpl3* mutants are more resistant to bacterial infection. Four-week-old plants were hand-inoculated with *Psm* at $OD_{600}=5 \times 10^{-4}$. The data are shown as means ± se with Student's *t*-test. * indicates $p<0.05$ compared to WT. **(E)** The *cpl3* mutants are more resistant to powdery mildew *Golovinomyces cichoracearum* UCSC1. The pictures were taken at 10 dpi on six-week-old plants. The numbers of spores per mg tissue (×1000) are shown on the top of the pictures. **(F)** Endogenous *FRK1* and *WRKY30* expression. The 12-day-old seedlings were treated with 100 nM flg22 for qRT-PCR analysis. The data are shown as means ± se from three biological repeats with Student's *t* -test. * indicates $p<0.05$ compared to WT.
The above experiments were repeated 3 times with similar results (see also Figure S2).

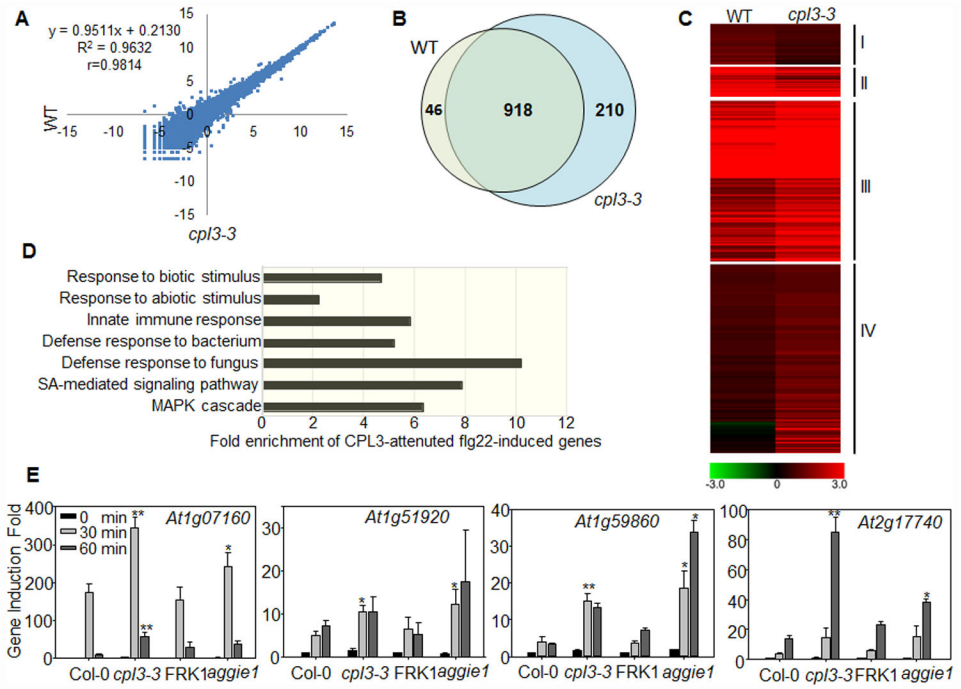

Figure 3. CPL3 globally regulates flg22-induced gene expression

(A) Scatter plot with the expression of whole genome transcripts between Col-0 (WT) and *cpl3-3* mutant. Twelve-day-old seedlings without treatment were used for analysis. y axis indicates gene expression in *cpl3-3*, and x axis indicates gene expression in WT. **(B)** Venn diagram of flg22-induced genes (fold change ≥ 2 and FDR < 0.05) in WT and/or *cpl3-3* seedlings 30 min after 100 nM flg22 treatment. **(C)** Heatmaps of CPL3-dependent flg22-induced genes. The four clusters are defined in the text. **(D)** Enrichment of defense-related genes in CPL3-attenuted flg22-induced genes (Group III). The fold enrichment was calculated based on the frequency of genes annotated to the term in Group III compared to their frequency in the genome. **(E)** qRT-PCR analysis of CPL3-regulated genes. The data are shown as means ± se from three biological replicates with Student's *t*-test. * indicates p<0.05, ** indicates p<0.01 compared to WT. (see also Figure S3, Table S1-S5).

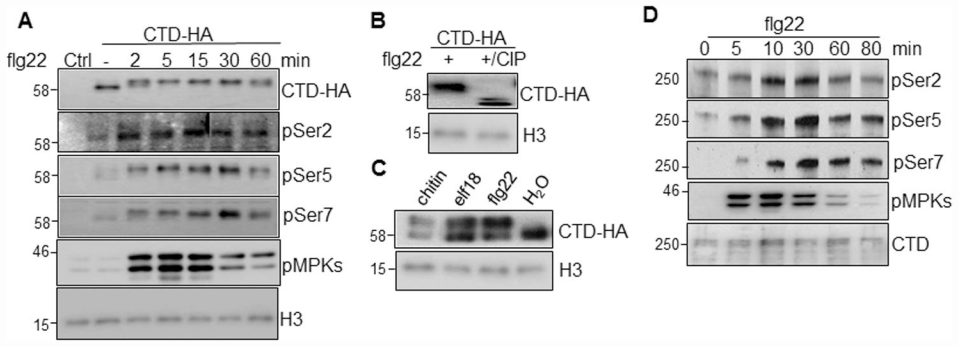

Figure 4. MAMPs induce CTD phosphorylation

(A) flg22 induces the mobility shift and phosphorylation of CTD in protoplasts. Protoplasts were expressed with CTD-HA, and stimulated with 100 nM flg22 for 2∼60 min. The proteins were analyzed by Western blot (WB) with α-HA, α-pSer2, α-pSer5, α-pSer7 or α-pERK antibody. The protein loading is shown by WB with α-Histone H3 antibody. **(B)** CIP treatment removes CTD-HA mobility shift. The flg22-stimulated protoplasts expressing CTD-HA were treated with 30 units of CIP at 37°C for 1 hr. **(C)** Different MAMPs induce CTD mobility shift in protoplasts. The CTD-HA transfected protoplasts were treated with 100 nM flg22 or elf 18 or 50 μg/ml chitin for 5 min. **(D)** flg22 induces endogenous CTD phosphorylation in *Arabidopsis* seedlings. Twelve-day-old seedlings were treated with 100 nM flg22 for indicated times, and the phosphorylation was detected with specific antibodies. The protein loading was shown by WB with α-CTD antibody.

The above experiments were repeated at least 3 times with similar results (see also Figure S4).

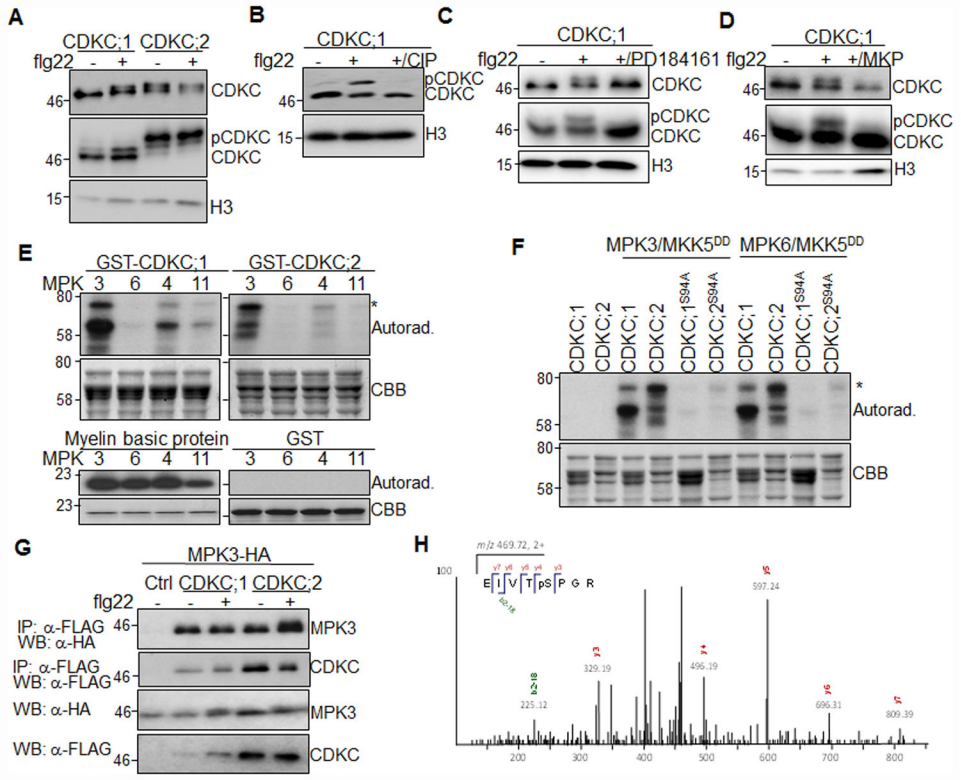

Figure 5. MAPKs phosphorylate CDKCs in flagellin signaling

(A) flg22 induces CDKC mobility shift in protoplasts. Protoplasts were expressed with CDKC; 1-HA or CDKC;2-HA and treated with 100 nM flg22 for 15 min. Total proteins were separated in a regular 10% SDS-PAGE gel (top) or supplemented with 50 μM phos-tag (Wako chemicals USA, Inc.) (middle). The loading control with α-H3 is shown on the bottom. **(B)** CDKC;1 mobility shift was removed by CIP treatment. Total proteins were separated in a SDS-PAGE gel supplemented with 50 μM phos-tag (top). **(C)** CDKC;1 mobility shift is blocked by MKK inhibitor PD184161 in protoplasts. 7.5 μM PD184161 was added 1 hr before flg22 treatment. **(D)** MAPK phosphatase (MKP) blocks CDKC;1 mobility shift. Protoplasts were co-expressed with CDKC;1-HA and MKP. In C & D, top is a regular SDS-PAGE and middle is phos-tag gel. **(E)** MPK3 phosphorylates GST-CDKC;1 and GST-CDKC;2 fusion proteins. FLAG epitope-tagged MPKs were expressed in protoplasts treated with 100 nM flg22, and immunoprecipitated for *in vitro* kinase assay with GST-CDKC;1 or GST-CDKC;2 as substrate. The reactions with myelin basic protein and GST protein as substrates are shown as controls. The protein loading of substrates is shown by CBB staining. **(F)** MPKs phosphorylate CDKCs at S94 *in vitro*. The recombinant HIS-MPK3 and HIS-MPK6 proteins were activated by constitutively active $MKK5^{DD}$, and used to phosphorylate GST-CDKCs and their S94A mutants. The phosphorylation was detected by autoradiograph and the protein loading is shown by CBB staining. * in E & F indicates the expected position of GST-CDKC. **(G)** CDKC;1 and CDKC;2 interact with MPK3 by Co-IP assay. FLAG epitope-tagged CDKC and HA epitope-tagged MPK3 were co-expressed in Col-0 protoplasts. The proteins were immunoprecipitated with α-FLAG agarose beads, immune-blotted with α-HA or α-FLAG antibody. The input of MPK3 and CDKCs is shown

by WB. **(H)** CDKC;1 S94 is phosphorylated by MPK3 as shown with MS analysis. The graph indicates the sequence of a doubly charged peptide ion at m/z 469.72 that matches to EIVTpSPGR of CDKC;1.

The above experiments (except MS assay) were repeated 3 times with similar results (see also Figure S5).

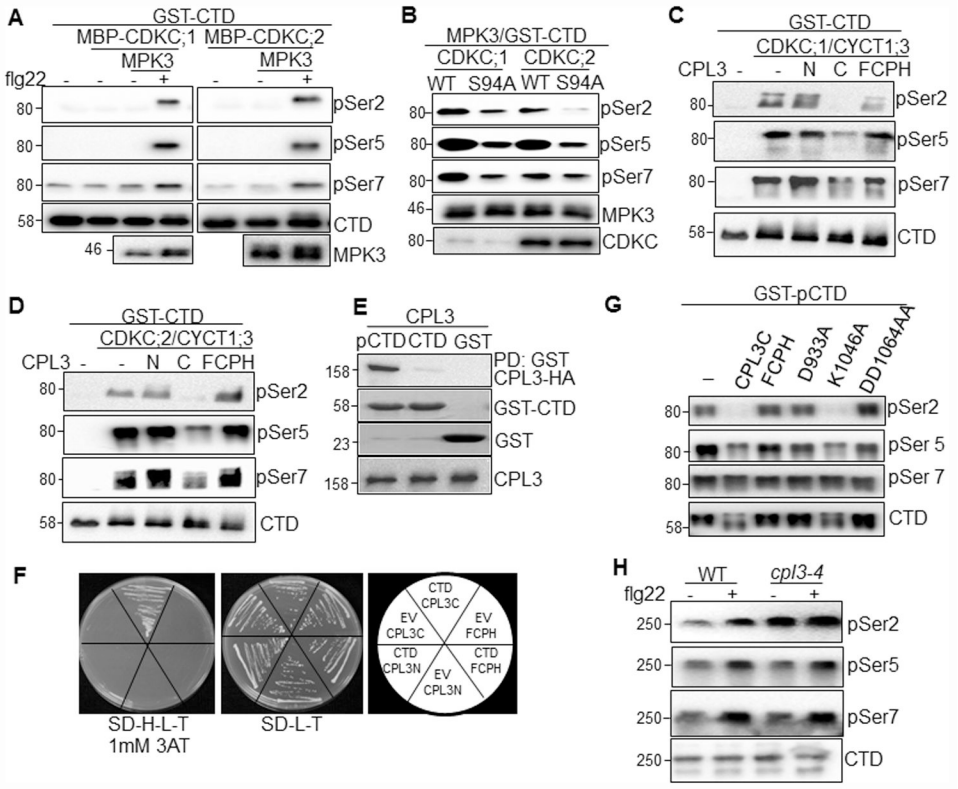

Figure 6. CPL3 is a CTD phosphatase

(A) MPK3-activated CDKCs induce GST-CTD phosphorylation *in vitro.* MPK3-HA was expressed in protoplasts treated with 100 nM flg22, immunoprecipitated with α-HA agarose beads, and incubated with MBP-CDKC proteins. The phosphorylated CDKC proteins were collected by centrifugation as supernatant (MPK3-HA conjugated beads were in pellets) and used to phosphorylate GST-CTD. The CTD phosphorylation was analyzed by WB with specific antibodies. **(B)** CDKC;1^{S94A} and CDKC;2^{S94A} reduce the ability to phosphorylate GST-CTD. **(C)** CPL3 dephosphorylates CDKC; 1-activated GST-CTD *in vitro.* CDKC;1-HA and CYCT1;3-HA were expressed in protoplasts, immunoprecipitated to phosphorylate GST-CTD. The phosphorylated GST-CTD was dephosphorylated by MBP-CPL3N (N), MBP-CPL3C (C) and MBP-FCPH. CTD phosphorylation was detected by WB with specific antibodies. CTD loading is shown by WB with α-GST antibody. **(D)** CPL3 dephosphorylates CDKC;2-activated GST-CTD *in vitro*. **(E)** CPL3 interacts with GST-CTD *in vitro.* Pull-down assay was performed by incubating MBP-CPL3 together with glutathione beads containing CTD or phosphorylated CTD (pCTD). The HA-tagged CPL3 proteins were detected with an α-HA WB after glutathione bead pull-down (PD). The input control is shown by WB. **(F)** CTD and CPL3C interact in yeast. The interactions between pGADT7-CTD and pGBDT7-CPL3C, pGBDT7-CPL3N and pGBDT7-FCPH were tested in SD medium without histidine, leucine and tryptophan (SD-H-L-T) supplemented with 1 mM 3AT. EV is the empty vector pGADT7. **(G)** CPL3C^{D933A} and CPL3C^{DD1064AA} lose phosphatase activity. **(H)** Enhanced CTD Ser2 phosphorylation in *cpl3-4* mutant seedling. One-week-old seedlings of WT and *cpl3-4* were treated with or without 1 μM flg22 for 30 min.

The above experiments were repeated 3 times with similar results (see also Figure S6).

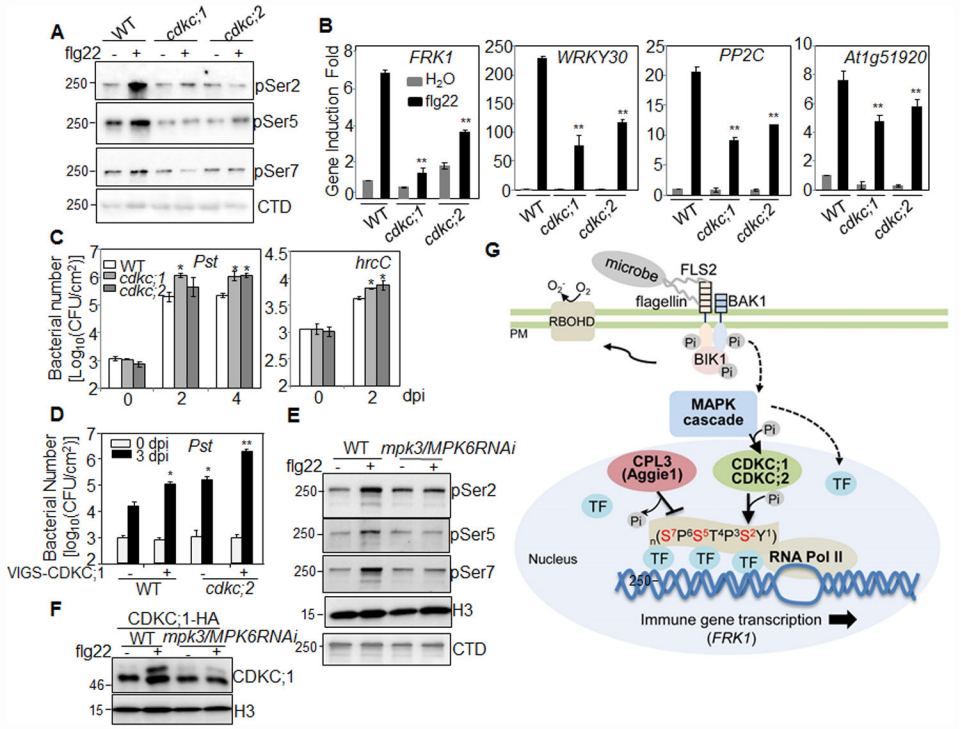

Figure 7. CDKCs positively regulate plant immunity

(A) CTD phosphorylation in *cdkc* mutants. One-week-old seedlings of WT, *cdkc;1RNAi (cdkc; 1*) and *cdkc;2* were treated with or without 1μM flg22 for 30 min. **(B)** flg22-induced gene expression. WT and *cdkc* seedlings were treated with 1 μM flg22 for 1 hr. **(C)** Bacterial growth in *cdkc* plants. WT and *cdkc* plants were hand-inoculated with *Pst* or *hrcC* at OD_{600} = 5×10^{-4}. **(D)** Bacterial growth in *CDKC* VIGS-silenced plants. The data in B, C and D are shown as mean ± se from three independent repeats with Student's *t*-test. * indicates $p<0.05$, and ** indicates $p<0.01$ compared to WT. **(E)** MPK3/6 are required for flg22-induced CTD phosphorylation. Protoplasts isolated from WT and *mpk3/MPK6RNAi* plants pretreated with 5 μM estradiol were treated with 100 nM flg22 for 15 min. **(F)** CDKC;1 mobility shift was partially blocked in *mpk3/MPK6RNAi* plants. Protoplasts were expressed with CDKC; 1-HA and treated with 100 nM flg22 for 15 min. Total proteins were separated in a 8% SDS-PAGE gel supplemented with 50 μM phos-tag. **(G)** A model of RNAPII CTD phosphorylation dynamics in plant immunity. Upon flg22 perception by the FLS2/BAK1/BIK1 receptor complex, rapid activation of MAPK cascade phosphorylates and activates CDKCs which further phosphorylate the tail of RNAPII CTD heptapeptide. The phosphorylation status of CTD is counter-regulated by CPL3 (Aggie 1) through direct dephosphorylation of the Ser residues on CTD. The phosphorylation dynamics of CTD serves as a "regulatory code" to recruit gene specific transcription factors (TFs) and orchestrate immune gene transcription.

The above experiments were repeated 3 times with similar results (see also Figure S7).